# Shear waves and shocks in soft solids

Hervé Tabuteau, Darek Sikorski, and John R. de Bruyn
*Department of Physics and Astronomy, University of Western Ontario, London, Ontario, Canada N6A 3K7*
(Received 28 July 2006; published 8 January 2007)

We study the motion of a sphere falling through soft viscoelastic materials when the time scale of the motion is short compared to the elastic relaxation time of the material. We observe shocks generated by the passage of the sphere at Mach numbers greater than 1. The sphere can undergo oscillations before reaching a steady terminal speed, and we show that these oscillations have the same frequency as the shear wave associated with the shock.

DOI: 10.1103/PhysRevE.75.012201 PACS number(s): 47.35.De, 83.60.Bc, 47.40.Nm

Viscous fluids do not support shear waves, but viscoelastic materials do. These shear waves propagate at a speed $c=(G/\rho_f)^{1/2}$, where $G$ is the elastic modulus and $\rho_f$ is the fluid density [1]. When the flow velocity $v>c$, shocks and a Mach cone will develop in viscoelastic materials [1], as has recently been observed experimentally [2]. This is not an exotic circumstance: in the materials we study here, $G$ is on the order of 100 Pa, so $c$ is a few tenths of a meter per second, orders of magnitude smaller than, for example, the speed of (longitudinal) sound waves in water [3]. This phenomenon is therefore expected to be important in many commonplace processes, including sedimentation and mixing of non-Newtonian fluids.

In this paper we study propagating disturbances generated by the motion of a sphere falling rapidly through shear-thinning viscoelastic materials. The Mach number $\mathrm{Ma}=v/c>1$ in most of our experiments. Experiments on the motion of spheres through viscoelastic fluids have shown that oscillations in the sphere's velocity can occur under certain conditions [4–8]. Underdamped periodic oscillations observed in elastic polymer solutions have been attributed to a competition between inertia and elasticity [5,9], while irregular, undamped oscillations observed in a solution of wormlike micelles [6] have been attributed to the effect of shear on the small-scale structure of the fluid [7,8]. Numerical simulations have been used to study the effects of system size and rheological parameters on these oscillations [10]. We show here that the oscillations of the falling sphere are related to shocks generated by the rapid motion of the sphere through the viscoelastic medium.

We studied several transparent, shear-thinning materials—a yield-stress fluid, a micellar fluid, and a physical gel—which have very different microstructures, but in all cases respond elastically at high frequencies, or, equivalently, on short time scales. Viscous and storage moduli were measured with an Ares RHS controlled strain rheometer using parallel plate tools with rough surfaces to prevent wall slip. Yield-stress gels were prepared using Carbopol ETD 2050 [11], a commercial polymer, at concentrations from 0.3 to 2.2 wt %. Samples were prepared by dispersing Carbopol powder in deionized water, adding 1$M$ NaOH to raise the $p$H to 6, then mixing thoroughly for up to one week, depending on concentration. The Carbopol dispersions behaved as soft elastic solids below their yield stress, and as shear-thinning viscoelastic fluids above. We take the elastic modulus $G$ for Carbopol as the low-frequency limit of the storage modulus [12]. An aqueous solution of wormlike micelles [13] was prepared by mixing 0.1 mol/l cetyltrimethylammonium bromide and 0.14 mol/l sodium salicylate in deionized water, stirring gently for a day, then leaving the solution to sit for one week at room temperature. This micellar fluid exhibited elastic behavior at high frequency and viscous behavior at low frequency. Its linear rheology was well described by a fit to a Maxwell model, from which $G$ and the relaxation time $\lambda=21$ s were obtained [14]. Finally, we used a 3 wt % solution of 2-hydroxyethyl cellulose (HEC, molecular weight $7.2\times10^5$ amu) in deionized water with 0.5 wt % sodium benzoate added as an antibacterial agent [15]. The ingredients were mixed for 4 h and the solution was then allowed to rest overnight at room temperature. HEC consists of linear polymer chains which entangle to form a physical gel and has a relaxation time $\lambda\approx2$ s. $G$ for HEC is taken to be the value of the storage modulus at the entanglement plateau exhibited at high frequencies [16,17].

The materials studied were contained in transparent Plexiglas or glass vessels having square cross sections of side $D$. Spheres of different densities $\rho_s$ and diameters $d$ were released from a holder carefully positioned a height $h$ above the center of the free surface, and hit the surface with a velocity $v_0=\sqrt{2gh}$, where $g$ is the gravitational acceleration. The experiments were recorded with a high-speed video camera, and the sphere's position in each video frame was obtained by image analysis. The complex phenomena associated with the impact itself will be discussed elsewhere [18]; here we are primarily concerned with what happens once surface effects are no longer important. The Deborah number $\mathrm{De}=2\lambda v_0/d$ is high for our experiments—for the wormlike micelles $1200<\mathrm{De}<12\,800$, and for HEC $62<\mathrm{De}<680$—indicating that the sphere moves through the material much more quickly than the elastic deformations can relax, so elastic effects will be important.

Figure 1 shows the trajectories of two different spheres falling through a Carbopol solution. For this material, $c=0.41$ m/s and Ma based on the impact velocity is greater than 1 for $h$ as small as 0.01 m. The less dense sphere slows and momentarily comes to rest at depth $z_p$ and time $t_p$, then rebounds and undergoes damped oscillations before eventually continuing to sink at a constant terminal speed [19]. The more dense sphere slows monotonically to its terminal speed; no oscillations are observed and $z_p$ is not defined in such cases. In Carbopol, a sufficiently light sphere will oscillate, then come to rest and remain suspended by the yield stress of the gel [20]. Neither the oscillations nor the phe-

 

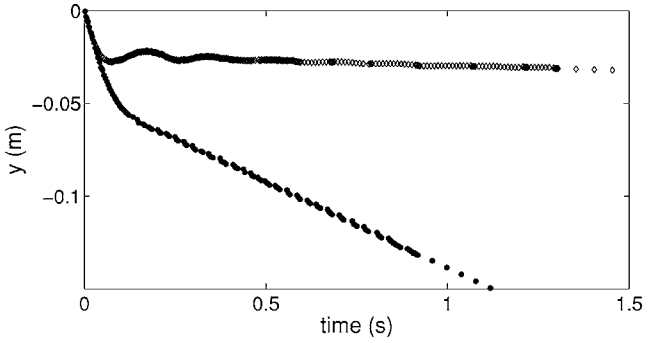


FIG. 1. The trajectories of a tungsten carbide sphere (solid circles, $\rho=15\,700$ kg/m$^3$, $d=0.0127$ m) and a chrome steel sphere (open diamonds, $\rho=7800$ kg/m$^3$, $d=0.0127$ m) released 0.03 m above a 2.2% Carbopol solution. The Mach number at impact is Ma=1.9.

nomena to be described below, however, depend on the yield stress—we observe similar oscillations in the wormlike micelle solution and, although more strongly damped, in HEC.

Both $z_p$ and $t_p$ increase with increasing impact velocity for a given material, and also depend on the properties of the fluid and on container size. With all other conditions fixed, both $t_p$ and $z_p$ increase linearly with $D$ for small containers, as shown in the inset to Fig. 2. In this regime, $t_p$ is approximately equal to the time it takes for the shear wave to travel the distance $D/2$ to the container walls. In larger containers, $t_p$ becomes constant.

$z_p/d$ is plotted as a function of the elastic Froude number $\mathrm{Fe}=(\rho_s-\rho_f)v_0^2/G$ [7] in Fig. 2. Data from experiments with all of the experimental fluids using spheres with $0.006\,25 \leq d \leq 0.0254$ m and $1400 \leq \rho \leq 15\,700$ kg/m$^3$ are shown. These measurements were made with $D$ large enough to avoid wall effects. The data collapse reasonably well onto a power law given by $z_p/d=(0.37\pm0.07)\mathrm{Fe}^{0.50\pm0.03}$.

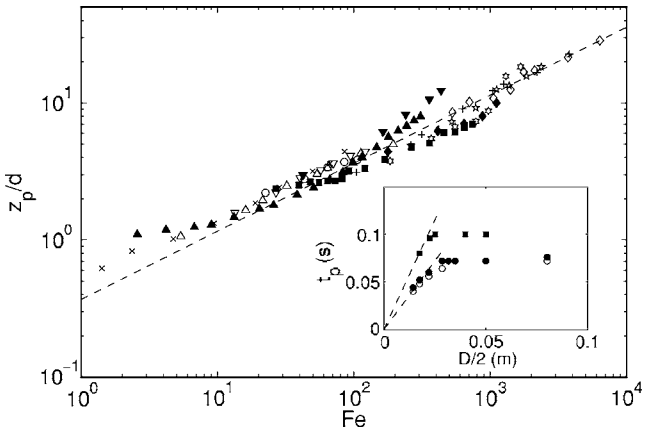


FIG. 2. The maximum penetration depth of the sphere before it rebounds $z_p$ scaled by the sphere diameter $d$, plotted as a function of the elastic Froude number defined in the text. The different symbols indicate data obtained with HEC (solid up and down triangles), wormlike micelles (solid circles and squares), and several concentrations of Carbopol (all other symbols), and with a variety of spheres of different densities and diameters. The dashed line is a power law fit to the data. The inset shows the rebound time $t_b$ as a function of container size for 1.2% Carbopol (open circles, $h=0.10$ m; solid circles, $h=0.40$ m) and wormlike micelles (solid squares, $h=0.39$ m). The dashed lines have slopes equal to $1/c$ for each material.

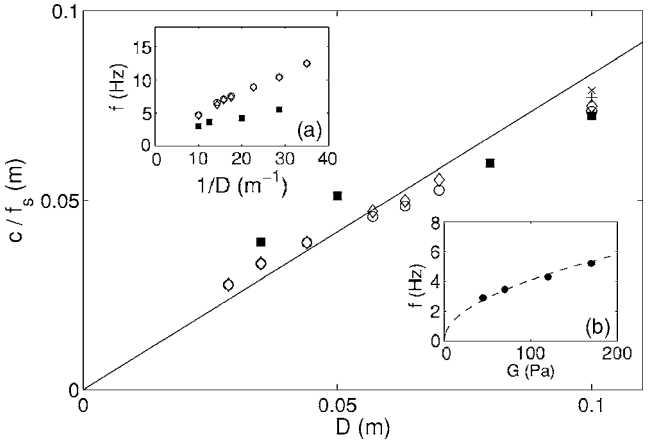


FIG. 3. Inset (a) The oscillation frequency $f_s$ of an aluminum oxide sphere ($d=0.0127$ m, $\rho_s=3950$ kg/m$^3$) as a function the reciprocal of the container size for 1.2% Carbopol with $h=0.40$ m (open circles) and 0.10 cm (open diamonds), and for a chrome steel sphere ($d=0.0127$ m, $\rho_s=7800$ kg/m$^3$) in the wormlike micelles with $h=0.39$ m (solid squares). Inset (b) $f_s$ as a function of $G$ for Carbopol solutions of different concentrations. The dashed line is a fit to a square-root dependence. Main figure: $c/f_s$ as a function of $D$. The symbols are as in (a), with the $\times$ being the mean of measurements for four different values of $\rho_s$ and the + the mean for four different Carbopol concentrations in the same container. The line is a fit to all of the data.

Although a power law exponent of 1/3 has been found from similar experiments with a different fluid [7], the $\mathrm{Fe}^{1/2}$ dependence observed here can be understood in terms of conservation of energy and without reference to any particular rheological model. Rearranging the expression for $z_p/d$ and solving for the initial kinetic energy of the sphere, we find $m_s v_0^2/2=m_f v_0^2/2+1.9G\pi z_p^2 d=m_f v_0^2/2+kz_p^2/2$, where $m_s$ and $m_f$ are the masses of the sphere and the corresponding volume of displaced fluid. We interpret this as an approximate energy budget for the system: the initial kinetic energy of the sphere is converted into kinetic energy of the fluid displaced as the sphere enters the fluid, plus elastic energy stored by deformation of the cylindrical volume swept out by the passage of the sphere; $k=3.8G\pi d$ is the equivalent of a spring constant.

The oscillation frequency $f_s$ of the sphere is independent of $d$, $\rho_s$, and $v_0$, but is inversely proportional to container size $D$, as shown in Fig. 3(a) for spheres in Carbopol and the wormlike micelle solution. $f_s$ shows an increase with $G$ that is consistent with a $G^{1/2}$ dependence, as shown in Fig. 3(b). When $c/f_s$ is plotted against $D$, as in the main plot of Fig. 3, the data for all materials collapse onto a straight line, with $c/f_s \approx D$. This suggests a connection between the oscillations of the sphere and a shear wave excited by the passage of the sphere through the viscoelastic material.

To visualize this wave directly, we positioned six 5 mm glass beads in a horizontal row 0.1 m below the surface of a Carbopol solution in a large ($D=0.25$ m) container, as illus-

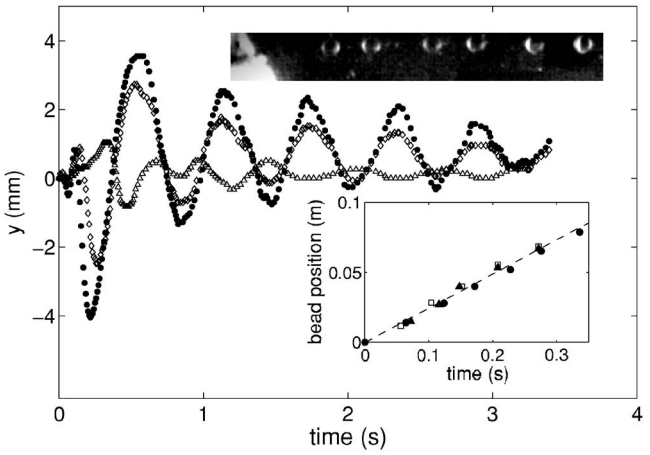


FIG. 4. The vertical position as a function of time of the first (solid circles), second (open diamonds), and sixth (open triangles) beads from a horizontal line of 0.005 m beads positioned close to the path of an impacting steel sphere with Ma$>1$. The material is 0.5% Carbopol. The upper inset shows the line of beads with the 0.0254 m sphere passing on the left-hand edge of the image. The lower inset shows the time of the first minimum in each bead's motion on the abscissa and the location of the bead on the ordinate. Here the different symbols indicate data from experiments with different falling spheres: squares, stainless steel, $\rho=7800$, $d=0.0254$ m; triangles, chrome steel, $\rho=7800$, $d=0.0127$ m; circles, acetal, $\rho=1400$, $d=0.0254$ m. The slope of the dashed line is the speed of the propagating disturbance.

trated in the upper inset to Fig. 4. The beads were prevented from sinking by the yield stress of the Carbopol. We then dropped a sphere with $v_0$ high enough that Ma$>1$ when it passed the line of beads and sufficiently dense that it reached the bottom of the container without undergoing any oscillations itself, and monitored the motion of the line of beads. When the sphere approaches the line of beads, the nearest bead is first pushed outward and then loops back in, following a roughly circular trajectory. This indicates a backflow vortex, which must be present due to the incompressibility of the fluid. The bead is then pulled downward and then oscillates vertically at a frequency $f_b$ as shown in Fig. 4. A short time later the second bead starts to oscillate at the same frequency, followed by the other beads in succession as they respond to a disturbance propagating radially outward. The lower inset to Fig. 4 shows the position of each bead in the line plotted against the time of the minimum in its vertical position. Data from experiments with three different spheres in the same material are shown. For 0.5% Carbopol, the slope of this plot gives a propagation speed of $0.244\pm0.008$ m/s, dependent only on the properties of the material and not on those of the falling sphere. This is in excellent agreement with the value of the shear wave speed $c=0.245$ m/s obtained from the measured elastic modulus.

Figure 5 shows results from a similar experiment using a less dense acetal sphere in the same Carbopol solution. In this case the projectile reaches $z_p$ and starts to oscillate at approximately the same depth as the row of smaller glass beads. After an initial transient, the sphere and the nearest bead oscillate in phase with $f_s=f_b$.

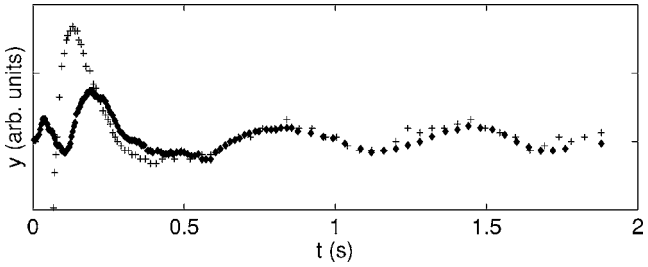


FIG. 5. The vertical position of a 2.54 cm acetal ball (crosses, $\rho=1400$ kg/m$^3$, $h=0.565$ m) undergoing oscillations in 0.5% Carbopol, and of the first bead (diamonds), located 0.14 m away at approximately the same depth. The data have been scaled and shifted vertically so that they superimpose. The sphere and the bead oscillate at the same frequency.

We do not observe waves excited by the sphere's passage in runs for which the terminal speed of the falling sphere is less than $c$. Since the shear waves themselves should exist for Ma$<1$, the disturbance we observe must in fact be the response of the material to the shock generated by the supercritical (Ma$>1$) motion of the sphere.

The oscillations of the beads persist for several seconds before being damped out, so the shock has time to reach the container walls and reflect back. While the beads closest to the falling sphere oscillate in phase with the sphere, those farthest away are out of phase, as shown in Figs. 4–6. Figure 6 shows the position of each bead at a sequence of times, and indicates a node close to the fourth bead, approximately 0.07 m $[(0.56\pm0.04)D]$ from the center of the container. Assuming an antinode at the center of the container where the impact occurs, this implies a standing wave with wavelength close to $2D$, consistent with the lowest normal mode of the square container.

We have studied phenomena associated with the motion of a sphere through viscoelastic materials on time scales short compared to the time scale for elastic relaxation in the materials. The depth to which the sphere penetrates before rebounding can be understood in terms of the conversion of kinetic energy into stored elastic energy. When Ma$>1$, shocks and elastic shear waves induced by the passage of the

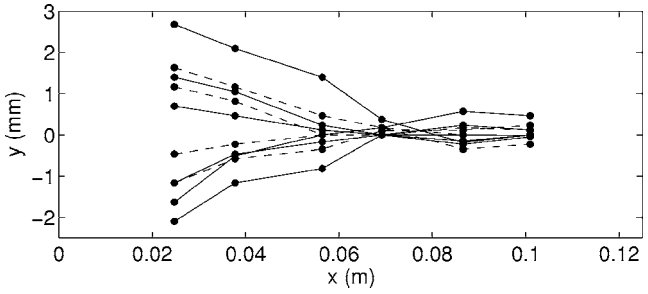


FIG. 6. The vertical position of each bead in a horizontal line of beads at several times following the passage of a sphere with Ma$>1$. The lines are guides to the eye which connect the points for a given time. The center of the falling sphere moved along $x=0$ and the container wall is at the right-hand edge of the figure.

sphere are observed whether or not the falling sphere undergoes oscillations, but when oscillations of the sphere are observed, they have the same frequency as the shear waves.

This research was supported by the Natural Science and Engineering Research Council of Canada. We acknowledge helpful discussions with P. Coussot.

[1] D. D. Joseph, *Fluid Dynamics of Viscoelastic Liquids* (Springer-Verlag, New York, 1990).
[2] S. Catheline, J. L. Gennisson, M. Tanter, and M. Fink, Phys. Rev. Lett. **91**, 164301 (2003); J. Bercoff, M. Tanter, and M. Fink, Appl. Phys. Lett. **84**, 2202 (2004).
[3] D. D. Joseph, O. Riccius, and M. Arney, J. Fluid Mech. **171**, 289 (1986).
[4] G. H. McKinley, in *Transport Processes in Bubbles, Drops, and Particles*, edited by R. P. Chhabra (Taylor and Francis, New York, 2002), p. 338.
[5] M. Arigo and G. H. McKinley, J. Rheol. **41**, 103 (1997).
[6] A. Jayaraman and A. Belmonte, Phys. Rev. E **67**, 065301(R) (2003).
[7] B. Akers and A. Belmonte, J. Non-Newtonian Fluid Mech. **135**, 97 (2006).
[8] S. Chen and J. P. Rothstein, J. Non-Newtonian Fluid Mech. **116**, 205 (2004).
[9] M. J. King and N. D. Waters, J. Phys. D **5**, 141 (1972).
[10] R. Zheng and N. Phan-Thien, Rheol. Acta **31**, 323 (1992); C. Bodart and M. J. Crochet, J. Non-Newtonian Fluid Mech. **54**, 303 (1994).
[11] http://www.pharma.noveon.com/literature/tds/tds216.pdf
[12] R. J. Ketz, R. K. Prud'homme, and W. W. Graessley, Rheol. Acta **27**, 531 (1988).
[13] M. E. Cates and S. J. Candau, J. Phys.: Condens. Matter **2**, 6869 (1990).
[14] M. Cloitre, T. Hall, C. Mata, and D. D. Joseph, J. Non-Newtonian Fluid Mech. **79**, 157 (1998).
[15] A. Maestro, C. González, and J. M. Gutiérrez, J. Rheol. **46**, 1445 (2002).
[16] R. G. Larson, *The Structure and Rheology of Complex Fluids* (Oxford University Press, New York, 1999).
[17] S. Ferree and H. W. Blanch, Biophys. J. **87**, 468 (2004).
[18] D. Sikorski, H. Tabuteau, and J. R. de Bruyn (unpublished).
[19] H. Tabuteau, P. Coussot, and J. R. de Bruyn (unpublished).
[20] A. Beris, J. A. Tsamopoulos, R. C. Armstrong, and R. A. Brown, J. Fluid Mech. **158**, 245 (1985).